Measuring Heterogeneous Uptake Coefficients of Gases on Solid Particle Surfaces with a Knudsen Cell Reactor: Complications Due to Surface Saturation and Gas Diffusion into Underlying Layers

P. Li,[†,‡] H. A. Al-Abadleh,[†] and V. H. Grassian*[,†,‡,§]

Departments of Chemistry and Chemical and Biochemical Engineering and the Center for Global and Regional Environmental Research, University of Iowa, Iowa City, Iowa 52242

Received: May 14, 2001; In Final Form: October 23, 2001

In this study, the complications and ramifications of surface saturation and gas diffusion in measuring heterogeneous uptake coefficients of gases on powdered samples with a Knudsen cell reactor are discussed. Computer simulations show that for uptake on a single layer, when coverage and surface saturation effects are included, the measured initial uptake coefficient will depend on the escape constant, k_{esc}, of the Knudsen cell reactor and is a lower limit of the true initial uptake coefficient. For powdered samples with many layers, it is shown that gases can readily diffuse into the bulk of the powder. In many cases, surface saturation and diffusion occur on the same time scale and contribute to the total overall observed uptake. A layer-by-layer model has been developed for gas uptake on powdered samples. The model takes into account gas diffusion into the underlying layers and surface saturation of each layer. The model is used to explain experimental results for heterogeneous uptake of trace atmospheric gases on oxide and carbonate powders that are often used as laboratory surrogates for mineral dust.

Introduction

Although its importance in stratosphere ozone depletion is firmly established, heterogeneous processes still represent one of the most uncertain areas in atmospheric chemistry, especially for those that occur in the troposphere.[1,2] In the troposphere, the role of mineral aerosol as a reactive surface in heterogeneous reactions of nitrogen oxides and volatile organics has been proposed to be important;[3] however, this hypothesis cannot be accurately assessed because the rates for many, if not most of these reactions, are unknown.

The Knudsen cell reactor has been widely used in determining the kinetics of heterogeneous processes since its introduction by Golden, Spoke, and Benson.[4] A Knudsen reactor is operated at very low gas pressures such that the mean free path of the gas is greater than the dimensions of the reactor and at least 10 times larger than the size of the exit aperture or escape hole. Thus, the gas-phase molecules in the reactor predominantly undergo collisions with the walls of the reactor, instead of collisions with each other. In this regime, termed the molecular flow regime, the kinetics of gas flow become very simple.

In the presence of a reactive solid substrate, a heterogeneous uptake coefficient, γ, can be derived under conditions of molecular flow and steady-state uptake.[4,5] The equation for this observed uptake coefficient, γ_{obs}, is

$$\gamma = \frac{A_h}{A_s}\frac{(N_0 - N)}{N} = \frac{A_h}{A_s}\frac{(I_0 - I)}{I} = \gamma_{obs} \qquad (1)$$

where A_h is the effective area of the escape hole or aperture, A_s is the geometric area of the sample holder, N_0 and N are the number of gas-phase molecules before and after the cover of the sample holder is opened to the solid substrate, respectively. N_0 and N are linearly proportional to the measured mass spectral ion intensity, I_0 and I, when a mass spectrometer is used to monitor reactant flow. This equation is typically applied in situations when the system is not at steady state.

The use of the geometric area of the sample holder, A_s, in calculating the observed uptake coefficient assumes that molecules collide only once and with the topmost layer of the sample. This is probably true if the sample is nonporous, e.g., a liquid or a continuous bulk solid sample where diffusion into the substrate does not occur. However, if the sample consists of a collection of particles in powdered form or some type of porous material, diffusion of gas molecules into the underlying layers and collisions with these internal surfaces will also contribute. The observed uptake coefficient, γ_{obs}, calculated via eq 1 will be larger than the true uptake as the amount of surface area sampled by the gas molecules is much larger than the geometric area of the sample holder. Therefore, the uptake coefficient calculated via eq 1 needs to be divided by a correction factor (n) to account for the actual surface area and the increase in the number of collisions that contributes to the overall uptake of molecules, i.e.

$$\gamma_t = \frac{\gamma_{obs}}{n} \qquad (2)$$

where γ_{obs} is defined in eq 1 and γ_t is the true uptake coefficient. The size of the correction factor will depend on the diffusion depth of the molecules into the powder. For high surface area powders, n will be quite large even when only a small amount of sample is used. For example, in a carbon black experiment where the geometric area of sample holder is 12 cm^2, 1 mg of carbon black (e.g., Degussa FW2 with a BET area of 460 m^2/g) will have a total BET area of 4600 cm^2. If all the BET area can be accessed by the gas molecules, then n is taken as the

* To whom correspondence should be addressed.
† Department of Chemistry.
‡ Center for Global and Regional Environmental Research.
§ Department of Chemical and Biochemical Engineering.

10.1021/jp011828q CCC: $22.00
Published on Web 01/25/2002

ratio of the accessible sample surface area to the geometric area and in this case is equal to 4600/12 = 383; i.e., the use of the sample holder geometric area in calculating γ can be over 2 orders of magnitude in error. However, it is not always easy to determine how much area has been accessed by the gas molecules, as this will depend on many factors including the diffusion constant of the gas into the powder, the surface area of the powder, and the true uptake coefficient, γ_t.

In 1991 Keyser, Moore, and Leu[6] proposed the use of a semiempirical model that had been developed for catalytic systems[7] to account for gas diffusion into porous samples of atmospheric relevance (herein referred to as the KML model). We have recently evaluated the application of the KML model to the uptake of gases on solid powdered samples.[8] It was found that the model is sometimes difficult to apply because the diffusion constant of the gas of interest through the powdered sample was a parameter in the model. Often the diffusion constant is unknown and difficult to measure or calculate. Sometimes an effective diffusion constant of a gas through a powdered sample is estimated from ideal gas behavior and the Knudsen diffusion constant. The Knudsen diffusion constant is calculated on the basis of the assumption that the molecules have zero residence time on the surface. However, it is clear from recent measurements of surface residence times by Koch et al.[19,20] that the assumption of zero surface residence time is not true for many molecules, especially for ones that are highly reactive or are considered "sticky", such as HNO_3.

In our earlier study,[8] we proposed an alternate way of applying the KML model by using a very small amount of sample mass to ensure that molecules diffusing into the powder can access the entire sample area. In this way, the total surface area of the sample, typically defined as the total BET surface area, can then be used to calculate the correction factor *n* without knowing the diffusion constant. It is easy to determine if the gas molecules are accessing the entire sample area by observing a linear mass dependence of γ_{obs}, the so-called "linear mass dependent" (LMD) regime. This method is found to be very effective for determining the true uptake coefficient for values of $\gamma_t \leq 1 \times 10^{-4}$ (note for $\gamma_t \leq 1 \times 10^{-4}$, γ_{obs} could be as high as 0.01). There are some difficulties and limitations in applying the LMD model if $\gamma_t > 1 \times 10^{-4}$ or the molecule is very sticky and the diffusion constant is low. First, it is difficult to prepare a sample in some cases when the LMD regime may require such a small sample mass (for example, mass < 1 mg) to be spread uniformly over the entire of sample holder area (typically between 5 and 15 cm^2). Second, the BET area of a powder sample is measured using nitrogen as the adsorbate. For porous particles, the internal pore areas accessible by nitrogen might not be accessible to larger molecules. Therefore, the correction by total BET area, even in the LMD regime will be too large. Third, the effects of surface saturation will artificially lower the experimentally determined uptake coefficient because by the time gas molecules diffuse into the deeper layers of a powdered sample the upper layers may already be saturated and thus chemically inactive. Surface saturation effects arise because there are a finite number of sites available for adsorption. When surface saturation occurs on a time scale similar to the response of the Knudsen cell reactor, there will be complications in measuring the initial uptake coefficient. These complications are addressed in detail here.

In this study, several issues concerning the measurement of uptake coefficients with a Knudsen cell reactor when the sample consists of many layers of particles are examined. First, the time-dependent behavior of Knudsen cell reactors is discussed. Second, the effects of surface saturation on a single layer are modeled. Third, for powdered samples a layer-by-layer model is developed that takes into account surface saturation of each layer and gas diffusion into the underlying layers. The model can be applied to the heterogeneous uptake of trace atmospheric gases on oxide and carbonate particles. These particles are often used as laboratory surrogates for mineral dust aerosol found in the troposphere.[8−17]

Results and Discussion

Time-Dependent Behavior of Knudsen Cell Reactors. Traditionally, the Knudsen cell reactor has been treated as a slow-response reactor because the total residence time for the average molecule in the Knudsen cell reactor is on the order of a few seconds and data collection times at intervals on the order of 3−5 s are typically used in these experiments. The Knudsen cell behaves like a well-stirred, continuous flow reactor, which means molecules entering the reactor chamber can achieve total mixing with the existing molecules in the reactor chamber in a period of time that is small compared to the total residence time.[4] Therefore, the initial response to the changes in pressure inside the reaction chamber is much quicker than the residence times of a few seconds.

Monte Carlo simulations by Fenter et al. showed that in some cases, this well-mixed state may not occur.[18] For example, when the Knudsen cell reactor is a long, narrow cylindrical tube that has a large exit aperture, the diffusion of gas molecules inside the tube will no longer be faster than the molecular effusion and a molecular density gradient occurs along the principal axis of the tube. Another case is when the Knudsen cell is used to measure heterogeneous uptake coefficients and the uptake coefficient is close to a value of 1. In this case, a local molecular density gradient will be created and the uniform distribution of gas molecules inside the Knudsen reactor is no longer valid.

In the following sections, we will discuss the response of a Knudsen cell reactor following an abrupt change in the gas pressure inside the reactor for four different cases. These four cases are shown schematically in Figure 1. Case A represents the situation where the flow out of the cell, F_{out}, is decreased by reducing the flow in, F_{in}. Here we will demonstrate that a change in the gas flow out of the cell can be closely monitored by a quadrupole mass spectrometer (QMS) and that the measured escape constant, k_{esc}, can be used to determine surface residence times on the walls of the reactor for any gas. Kinetic expressions are then derived for three cases involving heterogeneous uptake. Case B mimics heterogeneous uptake on a sample with an infinite number of surface sites such that surface coverage and saturation effects can be neglected. This is similar to monitoring the change in gas flow due to opening a second aperture with an area equal to the geometric area of the sample holder times the uptake coefficient, i.e., the fraction of collisions that lead to adsorption. Case C represents uptake on a bulk solid sample that consists of a single layer with a finite number of surface sites. In this case, surface coverage and saturation effects cannot be neglected and the uptake coefficient will be coverage and time dependent. Case D represents uptake on a powdered sample that consists of many layers. In this case, there will be uptake on the first layer and on the underlying layers of the powdered sample. Thus the time dependent diffusion of gas into the underlying layers needs to be taken into account. These four cases are presented in detail below. The ramifications of surface saturation, due to a finite number of surface sites, and gas diffusion, into the underlying layers of porous samples such as that is found for powdered samples, in determining heterogeneous uptake coefficients are discussed.

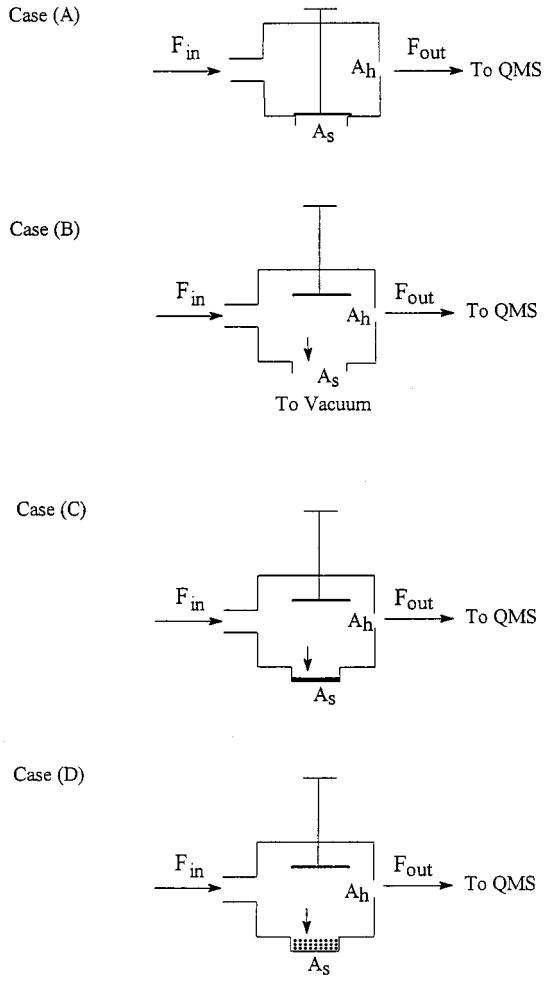

Figure 1. Several scenarios for a reduction in gas flow through the escape aperture (or escape hole), A_h. Each of the four cases is discussed in detail in the text. Case A: a reduction in gas flow, F_{out}, caused by a reduction in the inlet flow F_{in}. In this case, the sample holder cover is closed to the sample holder of area, A_s. Case B: a reduction in gas flow, F_{out}, caused by flow through a second aperture, A_s, or due to heterogeneous uptake in the absence of coverage and saturation effects. In this case (and in cases C and D), the sample holder cover is open to the sample. Case C: a reduction in gas flow, F_{out}, caused by heterogeneous uptake on a sample consisting of a single layer with a finite number of surface sites. Case D: a reduction in gas flow, F_{out}, caused by heterogeneous uptake on a powdered sample consisting of many layers of particles with a finite number of surface sites.

Case A: Response of the Knudsen Cell Reactor As Measured by a QMS; Decrease in Gas Flow Due to a Reduction in the Inlet Flow. Under the conditions of molecular flow used in a Knudsen reactor, collisions between molecules in the gas phase can be neglected and the total number of collisions that a molecule undergoes with the walls of the reactor before it exits through the escape aperture is simply the ratio of the total interior area of the reactor to the area of the escape aperture. Utilizing this characteristic of Knudsen flow, Koch et al. pioneered the molecular diffusion tube technique to measure the average surface residence time of molecules on the walls of the reactor.[19,20] A somewhat different approach to measuring surface residence times, τ_s, on the walls of the reactor is introduced here. However, the main purpose here is to obtain values of k_{esc}, the first-order escape constant, for different molecules.

When the sample holder is closed, a steady-state flow is established according to

$$F_{in} = F_{out} = k_{esc}N_0 \tag{3}$$

where F_{in} (molecule/s) is the flow in from the inlet, F_{out} (molecule/s) is the flow out of the chamber, N_0 is the number of molecules in the chamber, and k_{esc} (s^{-1}) is the first-order escape constant of molecules out of the reactor. When there are only elastic collisions between the molecules and the walls of the reactor, then ideal gas behavior is observed. In this case, there is no residence time on the walls and k_{esc} can be written as

$$k_{esc}^{ideal} = \frac{cA_h}{4V} \tag{4}$$

where A_h is the area of the escape aperture (cm^2), V is the volume of chamber (cm^3) and c is the mean molecular speed (cm/s) given by

$$c = \left(\frac{8 \cdot R \cdot T}{\pi \cdot M}\right)^{1/2} \tag{5}$$

where R is the gas constant, T is the temperature, and M is the molecular weight of the gas.

The residence time, τ_r, is defined as the first-order time constant and is given by

$$\tau_r = \frac{1}{k_{esc}^{ideal}} \tag{6}$$

For some molecules, the surface residence time on the wall, τ_s, is nonzero, thus the residence time will increase to

$$\tau_r = \frac{1}{k_{esc}^{ideal}} + \tau_s Z \tag{7}$$

where τ_s is the surface residence time of each individual molecular collision with the wall and Z is number of collisions an average molecule makes before it escapes out of chamber. Z can be calculated by

$$Z = \frac{A_r}{A_h} \tag{8}$$

where A_r (cm^2) is the total interior area of the reactor chamber.

The increase in τ_r, brought about by the nonzero surface-residence time, will reduce the measured escape constant, k_{esc}, relative to the ideal case and is equal to

$$k_{esc} = \frac{1}{\tau_r} = \frac{1}{\frac{1}{k_{esc}^{ideal}} + \tau_s Z} \tag{9}$$

One of the simplest methods for measuring k_{esc} is to first establish a steady-state flow, F_{in}. If F_{in} is suddenly reduced to F'_{in} a new steady-state flow will eventually reached, such that

$$F'_{in} = F'_{out} = k_{esc}N' \tag{10}$$

The rate of change between these two steady states can be described by

$$\frac{dN}{dt} = F'_{in} - F_{out} = F'_{in} - k_{esc}N = k_{esc}N' - k_{esc}N \tag{11}$$

This equation can be solved to yield

$$\ln\left(\frac{N - N'}{N_0 - N'}\right) = -k_{esc}t \quad (12a)$$

Plot $\ln((N - N')/(N_0 - N'))$ vs. t and the slope is $-k_{esc}$. If the QMS can follow the changes of pressure inside the chamber closely, N, N_0, and N' can be replaced by the corresponding QMS signal intensities I, I_0, and I′,

$$\ln\left(\frac{I - I'}{I_0 - I'}\right) = -k_{esc}t \quad (12b)$$

One way to verify whether substituting N with I is reasonable is to compare the measured k_{esc}, which is obtained from the plot of $\ln[(I - I')/(I_0 - I')]$ versus t, with calculated k_{esc}^{ideal} for a gas that behaves as an ideal gas and does not interact with the walls of the reactor. Molecular nitrogen at room temperature is such a gas, and k_{esc} and k_{esc}^{ideal} will be the same since surface residence time τ_s is zero. τ_s is calculated via

$$\tau_s = \frac{\dfrac{1}{k_{esc}} - \dfrac{1}{k_{esc}^{ideal}}}{Z} \quad (13)$$

Plots of of I vs t and $\ln[(I - I')/(I_0 - I']$ vs t for nitrogen are shown in Figure 2. Only the first 20 s are shown in Figure 2b as the data become noisy at longer times as they approach background levels of the $m/e = 28$ mass channel. Table 1 lists the calculated k_{esc}^{ideal}, the measured k_{esc}, and τ_s calculated via eq 13 for several molecules using the Knudsen cell reactor described in ref 12. As expected the residence time, τ_s, for molecular nitrogen on the walls of the reactor is 0. The N_2 data also show that the QMS can be used to accurately follow changes of the molecular density inside the reactor (i.e., the change of N vs t can be accurately represented by the change of the QMS intensity I vs t) and that k_{esc}^{ideal} is directly proportional to A_h, as expected. For the other molecules investigated, there are nonzero surface residence times. Note that these are surface residence times for molecules on the passivated stainless steel walls as the reactant gas passivated the system for several minutes to hours until a stable flow was achieved before each experiment. The largest surface residence time measured is 0.50 ± 0.10 ms for HNO_3. This value agrees well with that of Koch et al. who report a surface residence time for nitric acid on Teflon-coated stainless steel walls on the order of 0.5 ms and a larger residence time for nitric acid on uncoated stainless steel walls that were not previously passivated.[20]

It should be noted that there is some error in our measurements as the analysis does not take into account the fact that for molecules with nonzero residence times there will be molecules adsorbed on the walls of the reactor in equilibrium with the gas phase. The equilibrium between the gas phase and the molecules adsorbed on the walls of the reactor is affected by the change in the gas pressure. In the analysis of k_{esc}, only the very beginning portion of the natural log versus time graph was used, as it was found that the slope deviated from linearity as molecules desorb from the walls of the reactor at later times. However, wall effects are the most likely cause of the differences observed in the measured residence times between the two escape apertures. The main point of case A discussed above is that k_{esc} is less than the ideal value due to a nonzero residence time on the walls of the Knudsen cell reactor.

Case B: Response of the Knudsen Cell Reactor; Decrease in Gas Flow Due to Opening a Second Aperture to Vacuum (or Uptake on a Surface with an Infinite Number of Surface Sites). Before discussing heterogeneous uptake, we first discuss a hypothetical situation by assuming that the sample holder cover seals another escape aperture. The area of this second escape aperture (referred to as sample holder aperture hereafter) is the same as the geometric area of the sample holder, A_s (see Figure 1). This is equivalent to having a heterogeneous uptake of unity. When the sample holder cover is lifted, the flow out of the original escape aperture decreases to a new value, due to the branching between the sample holder aperture, A_s, and the original escape aperture A_h. Eventually, a new steady state will be established. The new steady state can be written as

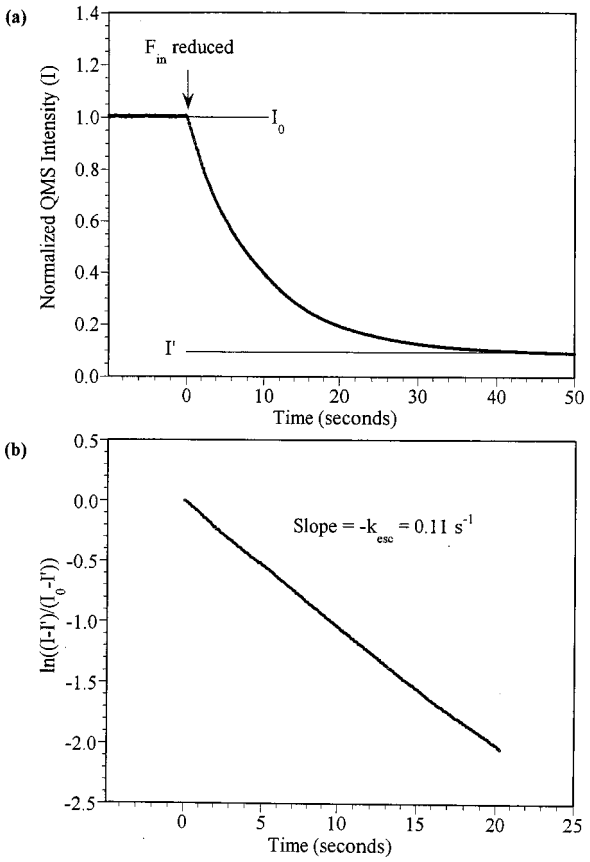

Figure 2. (a) Exponential decay of the normalized QMS signal (I) with time following an abrupt change in the inlet flow F_{in}. In this experiment, A_h is equal to 0.00724 cm^2. (b) Plot of $\ln[(I - I')/(I_0 - I')]$ versus time, where I_0 is the initial steady-state intensity before the flow was reduced and I' is the new steady-state intensity the system reaches. The slope of the plot is equal to $-k_{esc}$ (eq 12b). Table 1 lists the experimental values of k_{esc} and the inverse of k_{esc} and τ_s, the surface residence times, determined for several gases.

TABLE 1: Surface Residence Time of Various Molecules on the Walls of the Knudsen Cell Reactor (T = 295 K)

	A_h = 0.00724 cm^2			A_h = 0.0179 cm^2			
	$k_{esc}^{ideal\ a}$ (s^{-1})	k_{esc}^{b} (s^{-1})	τ_s^{c} (ms)	k_{esc}^{ideal} (s^{-1})	k_{esc} (s^{-1})	τ_s (ms)	average τ_s (ms)
N_2	0.11	0.11	0	0.27	0.27	0	0
CH_3COCH_3	0.075	0.067	0.013	0.19	0.17	0.013	0.013
NO_2	0.084	0.063	0.033	0.21	0.15	0.039	0.036
H_2O	0.13	0.022	0.32	0.33	0.058	0.29	0.31
HNO_3	0.072	0.012	0.58	0.18	0.040	0.40	0.50

[a] Ideal escape constant. [b] Measured escape constant. [c] Calculated surface residence time (see text for further details) using eq 13 with Z = 119,340 and 48,270 for A_h = 0.00724 cm^2 and 0.0179 cm^2, respectively.

$$F_{in} = F_{\text{sample holder}} + F'_{out} = \frac{A_s}{A_h} k_{esc} N + k_{esc} N \qquad (14)$$

The rate of change of the number molecules in the reactor between the original steady state and the new steady state can be expressed as

$$\frac{dN}{dt} = F_{in} - F_{\text{sample holder}} - F_{out} = k_{esc} N_0 - \frac{A_s}{A_h} k_{esc} N - k_{esc} N \qquad (15)$$

At steady state, this equation can be solved to yield

$$N = \frac{N_0}{\left(\frac{A_s}{A_h} + 1\right)} \qquad (16a)$$

In terms of mass spectral intensity, this equation becomes

$$I = \frac{I_0}{\left(\frac{A_s}{A_h} + 1\right)} \qquad (16b)$$

The discussion can be extended to the situation of heterogeneous uptake, that is, when the sample holder cover seals an adsorbent or reactive solid with an infinite number of surface sites. The adsorbent is acting as a vacuum pump and heterogeneous uptake is essentially similar to a sorption pump. The pumping efficiency of the adsorbent depends on the uptake coefficient, γ. Therefore, the rate of change between the two steady states becomes

$$\frac{dN}{dt} = k_{esc} N_0 - \gamma \frac{A_s}{A_h} k_{esc} N - k_{esc} N \qquad (17a)$$

and

$$\frac{dI}{dt} = k_{esc} I_0 - \gamma \frac{A_s}{A_h} k_{esc} I - k_{esc} I \qquad (17b)$$

If γ is a constant, at steady state eq 17 can be solved to yield a solution for γ

$$\gamma = \frac{A_h}{A_s}\left(\frac{N_0 - N}{N}\right) \qquad (18a)$$

and

$$\gamma = \frac{A_h}{A_s}\left(\frac{I_0 - I}{I}\right) \qquad (18b)$$

which is the same as eq 1.

The difference between eq 17 and eq 15 is the inclusion of γ in the middle term of the equation. This is mathematically equivalent to the sample holder aperture being reduced by a factor of γ; i.e., a value of $\gamma = 0.01$ can be interpreted, as only 1% of the sample holder aperture is effective.

Three simulated I vs t curves with γ equal to 0.01, 0.001, and 0.0001 are plotted in Figure 3a. These data are simulated using eq 17b. It is seen in Figure 3a that the higher the value of γ, the steeper the decay of I as a function of t. A point that needs to be emphasized is that when the sample holder cover is open, γ will step from zero to its constant value instantaneously, but the decay of I vs t (and N vs t) is gradual and continuous even though the opening of the sample holder aperture is sudden. As seen in Figure 3b, there is some delay time before the new steady state is reached and thus there is a delay time before the value of γ can be determined. This delay time will depend on the escape constant which for a given experimental apparatus is dependent on volume, V, and the escape hole or aperture, A_h through eq 4. Typically, for a given system k_{esc} is varied by changing A_h. This is shown in Figure 3c where three different escape apertures are used in the

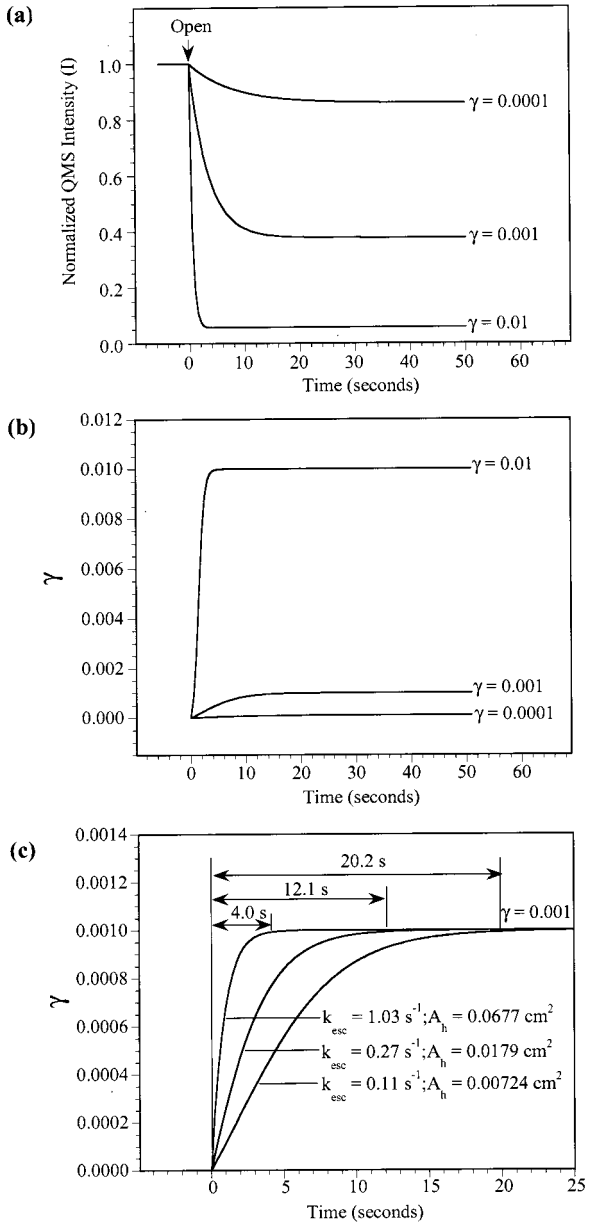

Figure 3. (a) Computer simulated normalized mass spectral intensity versus time traces for different values of the uptake coefficient, γ (γ = 0.01, 0.001, 0.0001). These data were simulated using eq 17b for each γ. The following experimental parameters, $k_{esc} = 0.11\ s^{-1}$, $A_h = 0.00724\ cm^2$, and $A_s = 11.95\ cm^2$ were used in the simulation. The arrow marked "open" is when the simulation begins. In an experiment, this is when the sample holder lid is open to the sample. (b) Uptake coefficient, γ, versus time plots for different values of the uptake coefficient. The uptake coefficient was calculated via eq 1 for each point in time using the simulated mass spectral intensity data shown in (a). (c) Calculated uptake coefficient, γ, versus time plots for a steady-state uptake coefficient of 0.001 as a function of the escape constant and escape aperture. Also given in the firgure is the time it takes for the uptake coefficient to reach 99% of its steady-state value is also shown.

simulation. The time it takes for the uptake coefficient to reach its steady-state value of 1×10^{-3} depends on the size of the escape aperture. The larger the escape aperture the faster the response of the reactor to changes in the gas concentration inside the reactor.

The main point of case B discussed above is to show that although the time it takes for the uptake coefficient to reach its steady-state value depends on k_{esc}, in the absence of surface saturation effects neither the value of the steady-state intensity nor the steady-state derived uptake coefficient is affected by k_{esc}.

Case C: Response of the Knudsen Cell Reactor; Decrease in Gas Flow Due to Uptake on a Surface with a Finite Number of Surface Sites (i.e., Including Surface Coverage and Saturation Effects). As discussed above for case B, when there are an infinite number of available surface sites, then the uptake coefficient determined from the Knudsen cell data is constant and independent of the escape constant. On a solid surface, this situation may be encountered for a catalytic reaction where sites are continuously regenerated. However, when adsorbed molecules block sites for further adsorption, there will be a time dependent uptake and the effects of surface coverage and saturation on the measured uptake coefficient will need to be determined. The effects of surface coverage and saturation on the measured uptake coefficient have not been previously considered for Knudsen cell experiments.

To initially simplify the discussion, we have assumed uptake on a single layer and consider the effects of surface coverage and saturation in determining initial uptake coefficients, γ_0, using a simple site-blocking, Langmuir-type adsorption mechanism.[21] In this case, the uptake coefficient is a function of coverage and takes the form

$$\gamma = \gamma_0(1 - \theta) \tag{19}$$

where γ is the uptake coefficient, θ is the surface coverage, and γ_0 is the uptake coefficient in the limit of zero surface coverage, i.e., $\theta = 0$. Assuming a first-order rate process in the gas pressure and the number of available surface sites $(1 - \theta)$, the rate of adsorption can be written as

$$\frac{dN_a}{dt} = k_a p N_s (1 - \theta) \tag{20}$$

where k_a is the rate constant for adsorption, p is the pressure of the gas, N_s is the total number of surface sites, and θ is the fractional coverage. If the pressure of the gas is taken to be nearly constant in this flow experiment (i.e., under conditions such that the change in the pressure is small), the rate of the reaction can be analyzed in terms of a pseudo-first-order process with respect to surface sites. With this assumption, and since $N = N_s\theta$ and $dN = N_s\, d\theta$, eq 20 can be solved and the solution of the differential expression is

$$(1 - \theta) = e^{-at} \tag{21}$$

where $a = k_a p$. Substituting eq 21 into eq 19 yields

$$\gamma = \gamma_0 e^{-at} \tag{22}$$

The rate of adsorption can also be written as

$$\frac{dN_a}{dt} = \gamma Z = \gamma \frac{p}{\sqrt{(2\pi mkT)}} = \gamma_0(1 - \theta)\frac{p}{\sqrt{(2\pi mkT)}} \tag{23}$$

where Z is the rate of collisions of the gas molecules with the unit surface area, m is the molecular mass, k is the Boltzmann constant, and T is the absolute temperature. By comparing eq 20 to eq 23, the rate constant becomes

$$k_a = \frac{\gamma_0}{N_s\sqrt{(2\pi mkT)}} \tag{24}$$

Therefore

$$a = k_a p = \frac{\gamma_0 p}{N_s\sqrt{(2\pi mkT)}} = 3.514 \times 10^{16}\frac{\gamma_0 p}{N_s\sqrt{MT}} \tag{25}$$

where p is in μTorr, N_s is in molecules cm^{-2}, M is the molar mass in g/mol, and T is the absolute temperature in K. Thus a depends on the initial uptake coefficient, the gas pressure, the average molecular velocity, and the number of available surface sites. Substituting eq 22 into eq 17 gives

$$\frac{dN}{dt} = k_{esc}N_0 - k_{esc}N - k_{esc}N\frac{A_s}{A_h}(\gamma_0 e^{-at}) \tag{26a}$$

and in terms of normalized mass spectral intensity this becomes

$$\frac{dI}{dt} = k_{esc}I_0 - k_{esc}I - k_{esc}I\frac{A_s}{A_h}(\gamma_0 e^{-at}) \tag{26b}$$

Since eq 26 cannot be analytically solved, it is numerically evaluated.

The effect of surface saturation on the calculated uptake coefficient is simulated in Figure 4a, where a series of intensity versus time traces as well as γ versus time curves with different values of the exponent a are presented. A value of $a = 0$ implies that there are no saturation effects corresponding to case B discussed. From eq 21, it can be seen that the larger the value of a, the faster the surface will saturate. The corresponding initial uptake coefficient γ_0 calculated via eq 1 is presented. The initial uptake is determined at the point in which I is at its minimum value, as is typically done in these experiments when steady-state conditions are assumed. It can be seen that only when there is no saturation effect, i.e., $a = 0$, does γ_0 calculated via eq 1 yield the value of 0.01 used in the simulation. The simulations using a time-dependent uptake coefficient, i.e., for $a > 0$, show that the observed initial uptake coefficient is always less than the actual initial uptake coefficient and is thus a lower limit to the true uptake coefficient γ_0. The reason for this is that when there is a coverage dependence due to a finite number of available surface sites then I (or N) is unable to reach its steady-state value assumed in the derivation of eq 1. Therefore, γ_0 calculated via eq 1 is only a lower limit because the surface coverage increases on the time scale of the experiment.

As shown and discussed in the previous section, when eq 1 is valid and there are no coverage effects, then the calculated uptake coefficient will be independent of the escape constant and the size of the escape aperture, A_h. However, when the uptake coefficient depends on surface coverage, it is found that the experimentally determined initial uptake coefficient, γ_0, depends on k_{esc} and for a given experimental system of fixed volume depends on A_h. Computer simulations demonstrating this point are shown in Figure 4b. This is an example where the surface saturates quickly ($a = 5.0$). It can be seen in Figure 4b that the observed initial uptake coefficient calculated via eq 1 for a single layer is dependent on the escape constant and escape aperture. Although always lower, the value of γ_0 calculated from the data approaches the true value of the initial

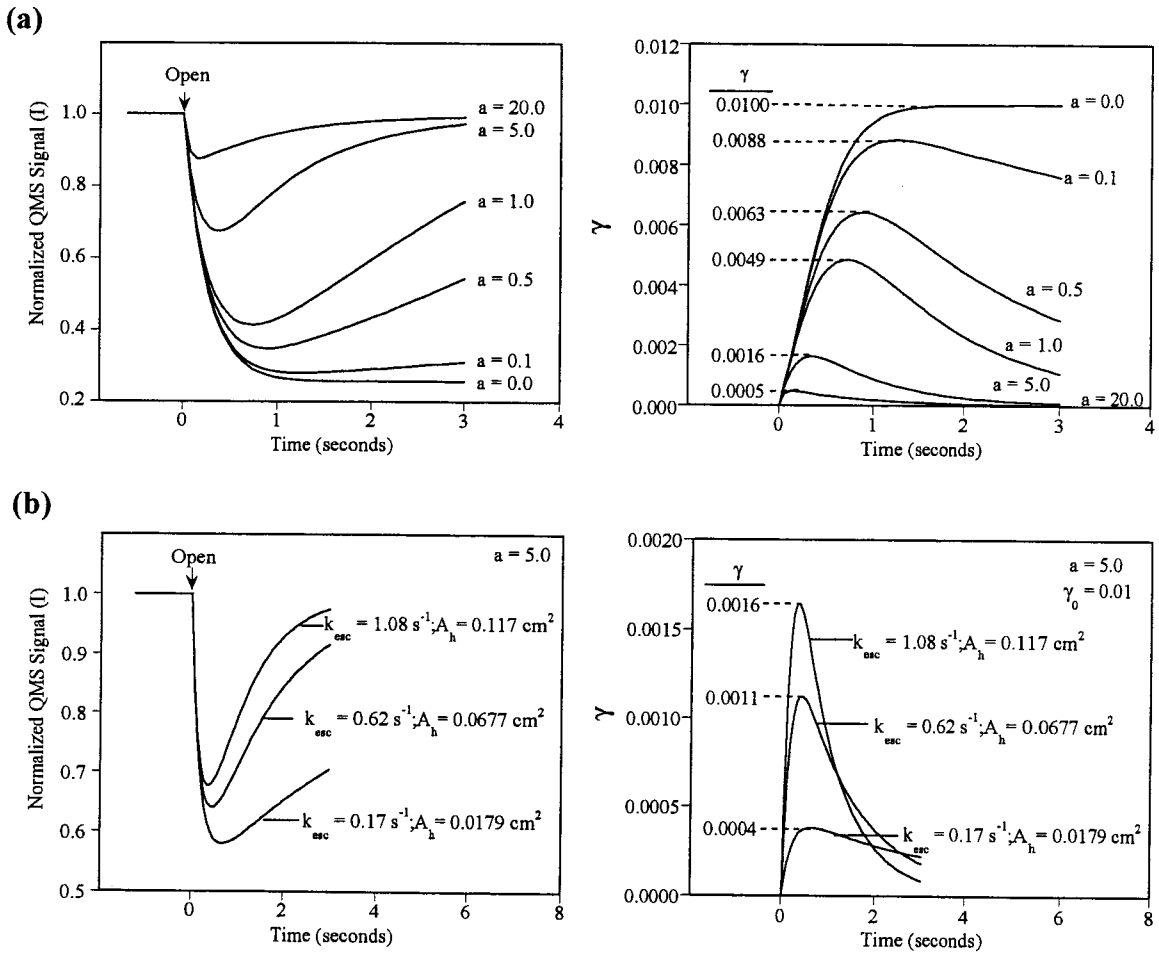

Figure 4. (a) Computer simulated normalized mass spectral intensity versus time traces showing the effects of surface coverage and saturation. These data were simulated by numerical evaluation of eq 26b with the following experimental parameters, $k_{esc} = 1.08\ s^{-1}$, $A_h = 0.117\ cm^2$, and $A_s = 33.98\ cm^2$. Computer simulations for an initial uptake coefficient, γ_0, equal to 0.01 are shown for different surface saturation effects, as determined by the parameter a ($a = 0.0$, 0.1, 0.5, 1.0, 5.0, 20.0). For a equal to 0 there are no surface coverage and saturation effects. Uptake coefficient, γ, versus time plots are also shown. The uptake coefficient was calculated via eq 1 for each point in time using the simulated mass spectral intensity data. (b) Computer simulated normalized mass spectral intensity versus time traces showing the dependence on escape apertures, A_h, and thus k_{esc} values, when there are surface coverage and saturation effects. These data were simulated by numerically evaluating eq 26b with the following experimental and input parameters, $a = 5.0$, $\gamma_0 = 0.01$, $A_s = 33.98\ cm^2$, and different $A_h = 0.0179$ ($k_{esc} = 0.17\ s^{-1}$), 0.0677 ($k_{esc} = 0.62\ s^{-1}$), and 0.117 cm^2 (1.08 s^{-1}). Uptake coefficient, γ, versus time plots are also shown. The uptake coefficient was calculated via eq 1 for each point in time using the simulated mass spectral intensity data.

uptake coefficient as k_{esc} increases. The shapes of the intensity versus time and γ versus time curves also change. For the larger aperture, the curves are narrower with a more well-defined maximum for γ and a more well-defined minimum for the mass spectral intensity. The reason for this is that the response of the Knudsen cell reactor is faster when using a larger aperture. However, the sensitivity of the Knudsen cell reactor is less when a larger escape aperture is used, i.e., $I_0 - I$ decreases with increasing aperture size. The conclusion that can be made from the model and simulations presented in case C is that when there are surface coverage and saturation effects, the initial uptake coefficient calculated via eq 1 is a lower limit.

It should be noted that in the above discussion the adsorption process was taken as irreversible and a simple Langmuir-type site blocking mechanism, i.e., a $(1 - \theta)$ dependence, was used to describe the coverage effect on the observed uptake coefficient. This type of mechanism has been shown to be operative in the heterogeneous uptake of nitric acid on NaCl.[22] There are other coverage dependencies observed, including some that are exponential, $e^{-\theta}$.[21] In the case of precursor-mediated adsorption, there is little coverage dependence on the uptake coefficient, γ, until a coverage near 0.5, and then γ decreases quickly.[21]

Case D: Response of the Knudsen Cell Reactor; Decrease in Gas Flow Due to Uptake on a Powdered Sample Consisting of Many Layers and a Finite Number of Surface Sites (i.e., Including Surface Coverage and Saturation Effects as Well as Gas Diffusion into Underlying Layers). For heterogeneous uptake on powdered samples, the uptake coefficient is time dependent due to surface saturation and gas diffusion into the underlying layers of the sample. If the Knudsen cell reactor is to be used to determine accurate kinetic data for heterogeneous reactions on solid particles, then the time-dependent uptake coefficient needs to be taken into account. Therefore, the cases detailed above (cases B and C) serve as an introduction to the discussion for measuring heterogeneous uptake on powdered samples. To understand how γ changes with time, the possible pathways an incoming gas phase molecule can take when the sample holder is opened is illustrated in Figure 5. An incoming molecule can collide with the first layer of particles of the powdered sample or diffuse through the void region between the particles and then adsorb on the surface of the particles in the underlying layers. The uptake on the first layer can potentially occur at a faster rate compared to the uptake on the underlying layers, since gas

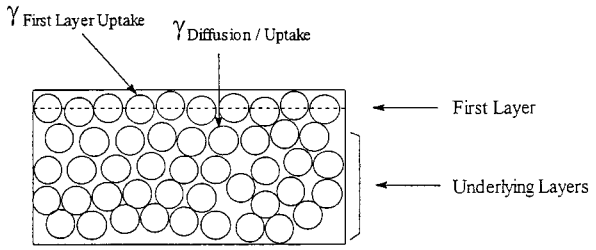

Figure 5. Possible pathways a gas reactant molecule can take upon opening the sample holder cover containing a powdered sample. These pathways include uptake on the first layer of particles, diffusion into the powder, and uptake on the underlying layer of particles.

diffusion through the sample will take some time that depends on the diffusion constant and the thickness of the sample. For many molecules, the time scale for diffusion and uptake is similar and so these processes need to be considered in a simultaneous coupled manner.

A powdered sample consists of many layers of particles. Here we develop a layer-by-layer approach to describe the uptake of a gas by a porous solid. The uptake on each of the individual layers can be described by eq 21, but the gas molecules do not reach all the individual layers at the same time due to the diffusion time through the powder. The first layer is unique because there is no diffusion time in the powder.

The uptake can be described for each layer as follows

$$\text{First Layer: } \gamma_1 = \gamma_0 e^{-at}$$

$$\text{Second Layer: } \gamma_2 = \begin{cases} \gamma_0 e^{-a(t-t_2)} & \text{if } t \geq t_2 \\ 0 & \text{if } t < t_2 \end{cases}$$

$$\text{Third Layer: } \gamma_3 = \begin{cases} \gamma_0 e^{-a\cdot(t-t_3)} & \text{if } t \geq t_3 \\ 0 & \text{if } t < t_3 \end{cases}$$

$$\cdots$$

$$n\text{th Layer: } \gamma_n = \begin{cases} \gamma_0 e^{-a\cdot(t-t_n)} & \text{if } t \geq t_n \\ 0 & \text{if } t < t_n \end{cases} \quad (27)$$

where t_2 is the time it takes for gas molecules to diffuse to the second layer, t_3 is the time to get to the third layer, etc. If at any time $t < t_n$, i.e., before the gas molecules can reach the nth layer, there is no uptake on that layer so the uptake coefficient is set equal to zero. After the gas molecules reach the layer, the uptake process follows eq 21.

The time it takes to get to each layer can be determined from the diffusion time through the powder. The root-mean-square distance l traveled by molecules with effective diffusion constant D_{eff} in time t is given by[23]

$$l = \sqrt{2D_{\text{eff}}t} \quad (28)$$

Therefore, the time it takes to diffuse is

$$t = \frac{l^2}{2D_{\text{eff}}} \quad (29)$$

For a powder sample with mass m_s and powder density ρ packed in a sample holder with geometric area A_s, the total thickness, L, is given by

$$L = \frac{m_s}{\rho_b A_s} \quad (30)$$

If the specific BET area of the powder sample is S_{BET}, the total BET area of the powder sample is $m_s S_{\text{BET}} = A_{\text{BET}}$; the whole powder sample can then be treated as j layers of A_s surfaces stacked one on top of the other with

$$j = \frac{A_{\text{BET}}}{A_s} \quad (31)$$

and the distance between two adjacent A_s surfaces is

$$d = \frac{L}{j} \quad (32)$$

The incorporation of saturation and diffusion into eq 26 is then straightforward and the Knudsen cell equation in terms of the mass spectral intensity becomes[24]

$$\frac{dI}{dt} = k_{\text{esc}}I_0 - k_{\text{esc}}I - k_{\text{esc}}I\frac{A_s}{A_h}\{\sum_{i=0}^{j}\gamma_0\xi_t\}$$

$$\xi_t = \begin{cases} e^{-a\cdot[t-(i/jL)^2/2D_{\text{eff}}]} & \text{if } t \geq \dfrac{\left(\frac{i}{j}L\right)^2}{2D} \\ 0 & \text{if } t < \dfrac{\left(\frac{i}{j}L\right)^2}{2D} \end{cases} \quad (33)$$

where

$$i = n - 1 \quad (34)$$

and

$$t_i = \frac{\left(\frac{i}{j}L\right)^2}{2D_{\text{eff}}} \quad (35)$$

Although gas diffusion through the powder is treated in a rather simple fashion here, eq 33 can be used to model the experimental observations such as the mass and time dependence of the observed uptake as well as the pressure dependence.[16] Consideration of a distribution of pressures through the powder gave similar results.[25]

In eq 33, the initial uptake coefficient, γ_0, and the effective diffusion constant, D_{eff}, are fitting parameters. Most other parameters in the equation are experimental parameters (pressure, k_{esc}, ρ, A_s, A_{BET}, *and* mass). The number of surface sites, N_s, as defined in eq 20, can be determined from the experimental data if the experiment is done such that the QMS intensity is calibrated to flow (molecules s^{-1}) and the experiment is done until the surface is completely saturated. Thus a plot of the number of molecules that reacted per unit time integrated over time will yield the total number of molecules reacted. The coverage in units of molecules cm^{-2} is then determined from the total number of molecules adsorbed divided by the entire surface area of the powder.[14]

It is instructive to look at some limiting cases and an intermediate case. The first case is when diffusion is slow and the uptake coefficient is large. In this case, as D_{eff} approaches zero, t_i, the time it takes to diffuse to underlying layers, goes to infinity. Thus, the uptake occurs on the top layer only. The second case is for fast diffusion, as expected when the uptake coefficient is small. In this case, as D_{eff} becomes very large, then the second term in the exponential goes to zero. The entire bracketed part of eq 33 then reduces to $jA_s\gamma_o e^{-at} = A_{\text{BET}}\gamma_o e^{-at}$; thus all internal layers are simultaneously contributing to the

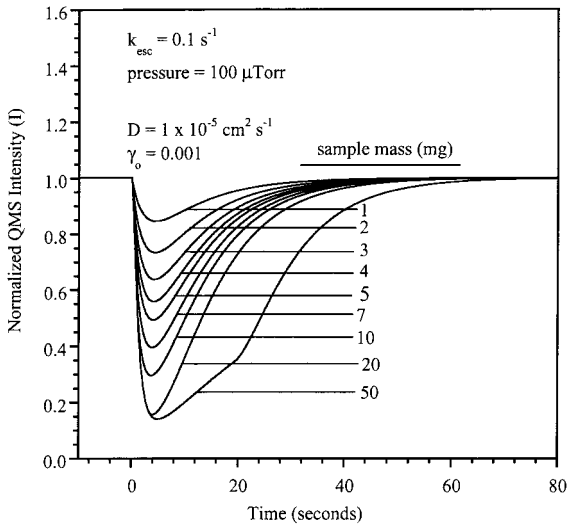

Figure 6. Computer simulated normalized mass spectral intensity (I) curves versus time as a function of mass. This simulation represents an intermediate case such that heterogeneous uptake and gas diffusion occurs on the same time scale. The simulation was done using the parameters given in Table 2b and the layer-by-layer uptake model (eq 33) discussed in the text.

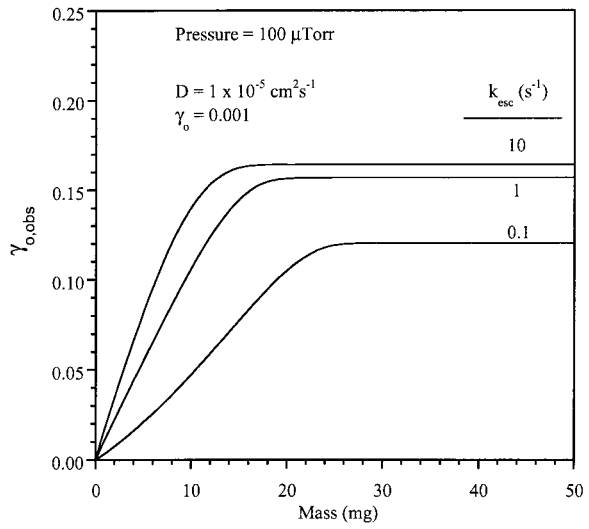

Figure 7. Computer simulated $\gamma_{o,obs}$ (calculated using eq 1) versus mass plots from the data presented in Figure 6 and some additional simulated time-dependent mass normalized mass spectral intensity curves for larger masses and for different escape constants. This simulation shows that the heterogeneous uptake depends on the escape constant of the Knudsen cell reactor.

TABLE 2: Parameters Used in the Simulation of the Layer-by-Layer Uptake Model (T = 295 K)

experimental parameters	
A_s (cm^2)	5.07
A_h (cm^2)	0.10[a]
k_{esc} (s^{-1})	0.10[a]
S_{BET} (cm^2 mg^{-1})	100
ρ (g cm^{-3})	0.5
M (g mol^{-1})	28
P (μTorr)	100[a]
N_{max}	1×10^{14}
D_{eff} (cm^2 s^{-1})	1.0×10^{-5}
γ_o	0.001

[a] Parameters varied; see text for further details.

uptake. This typically occurs for uptake coefficients that are $\leq 10^{-4}$, as found for SO_2 uptake on MgO and α-Al_2O_3.[15]

The heterogeneous uptake of HNO_3 on α-Al_2O_3 and $CaCO_3$ represents an intermediate case where diffusion and saturation occur on the same time scale.[13,16] Intermediate cases will involve diffusion and surface saturation occurring on the same time scales. An intermediate case is simulated to show some important consequences when diffusion and surface saturation occur on the same time scale.

Figure 6 shows computer simulated data as a function of sample mass for $\gamma_o = 0.001$. The other parameters used in the simulation are listed in Table 2. It can be seen from the simulated data that all of the underlying layers are being accessed during the course of the experiment. The computer simulated data show that the maximum in the observed uptake is dependent on mass and shifts to longer times with increasing mass and thus the number of layers of particles. An interesting consequence of this intermediate case is that surface saturation and gas diffusion occur on similar time scales and there is a significant dependence on k_{esc} similar to what is observed for uptake on a single layer. The maximum in the observed uptake, calculated via eq 1 and taken as the initial uptake coefficient, as a function of sample mass for four different escape constants is shown in Figure 7. For the smallest k_{esc}, the value of $\gamma_{o,obs}$ is lower and the linear range extends out further to larger masses. For each escape constant, the value of the true initial uptake coefficient $\gamma_{o,t}$ determined using the LMD regime is below the true initial uptake coefficient of 0.001 used in the simulation. For k_{esc} of 10 s^{-1}, the uptake coefficient calculated using the LMD regime is 7.8×10^{-4}. For k_{esc} of 0.1, the uptake coefficient calculated using the LMD regime is lower, 2.8×10^{-4}, nearly 4 times lower than the true initial uptake coefficient. Thus, the computer simulated data show that when saturation effects are important, the calculated uptake coefficient using the LMD regime is a lower limit to the true uptake and more accurate values of γ_o determined from the LMD regime are obtained when larger escape apertures and thus larger values of k_{esc} are used.

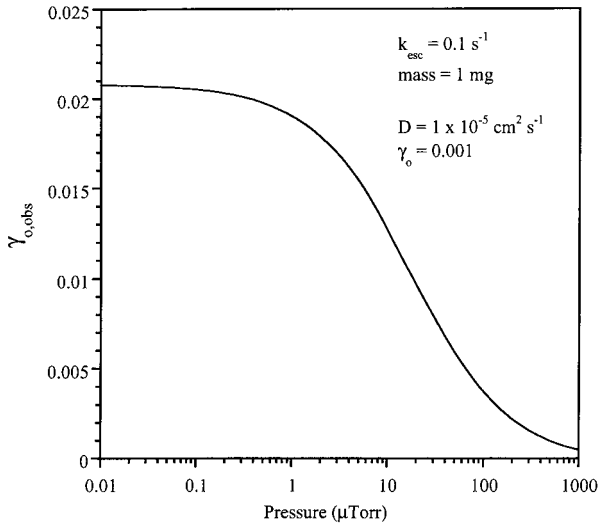

Figure 8. Computer simulated $\gamma_{o,obs}$ (calculated using eq 1) versus pressure plot.

From eqs 25 and 33, it is also seen that the pressure may have an effect on the measured initial uptake coefficient, i.e., higher pressures will show larger saturation effects. This is because each layer will saturate quickly on the time scale of the measurement. The pressure dependence for the computer simulated intermediate case is shown in Figure 8. The shape of the curve is similar to what has been reported in ref 13 for HNO_3 uptake on $CaCO_3$ and in ref 14 for NO_2 uptake on α-Al_2O_3.

Conclusion

In this study, we have considered the complications and ramifications due to surface saturation and gas diffusion when measuring the irreversible heterogeneous uptake of gases on solid particle surfaces using a Knudsen cell reactor. It is shown that in the presence of coverage and saturation effects the measured initial uptake coefficient corrected for surface area will be a lower limit to the true uptake coefficient and will depend on the escape constant of the Knudsen cell reactor. These effects are important for uptake on a single layer as well as for powdered samples that consist of many layers. When saturation effects are important and when considering the time scale of the measurement, it is difficult to determine an accurate value of the initial uptake coefficient. For powders, diffusion of the gas molecules into the underlying particle layers contributes to the overall observed uptake. The linear mass dependent regime depends on k_{esc} and is smallest for larger escape constants. The uptake coefficient using the LMD regime will be a lower limit to the true uptake coefficient. Large escape constants give most accurate values of the initial uptake coefficient.

Acknowledgment. We gratefully acknowledge the Department of Energy-Atmospheric Chemistry Program (DE-FG02-98ER 62580) and the National Science Foundation (CHE-9988434) for support of this work. We thank Professor Barbara J. Finlayson-Pitts for providing us with preprints prior to publication.

References and Notes

(1) Kolb, C. E.; Worsnop, D. R.; Zahniser, M. S.; Davidovits, P.; Keyser, L. F.; Leu, M.-T.; Molina, M. J.; Hanson, D. R.; Ravishankara, A. R.; Williams, L. R.; Tolbert, M. A. In *Progress and Problems in Atmospheric Chemistry*; Advances in Physics and Chemistry Series. 3; Barker, J. R., Ed.; World Scientific: Singapore and River Edge, NJ, 1995; Chapter 18.

(2) DeMore, W. B.; Sander, S. P.; Golden, D. M.; Hampson, R. F.; Kurylo, M. J.; Howard, C. J.; Ravishankara, A. R.; Kolb, C. E.; Molina, M. J. In *Chemical Kinetics and Photochemical Data for Use in Stratospheric Modeling*; JPL Publication 97-4; JPL: Pasadena, CA, 1997; pp 220−255.

(3) Dentener, F. J.; Carmichael, G. R.; Zhang, Y.; Lelieveld, J.; Crutzen, P. J. *J. Geophys. Res.* **1996**, *101*, 22869.

(4) Golden, D. M.; Spokes, G. N.; Benson, S. W. *Angew. Chem., Int. Ed. Engl.* **1973**, *12*, 534.

(5) Golden, D. M.; Manion, J. A.; Reihs, C. M.; Tolbert, M. A. In *The Chemistry of the Atmosphere: Its Impact on Global Change*; Calvert, J. G., Ed.; Blackwell Scientific Publications: Oxford, U.K., 1994.

(6) Keyser, L. F.; Moore, S. B.; Leu, M.-T. *J. Phys. Chem.* **1991**, *95*, 5496.

(7) Aris, R. The *Mathematical Theory of Diffusion and Reaction in Permeable Catalysts*; Clarendon Press: Oxford, U.K., 1975; Vol. I.

(8) Underwood, G. M.; Li, P.; Usher, C. R.; Grassian, V. H. *J. Phys. Chem. A* **2000**, *104*, 819.

(9) Borensen, C.; Kirchner, U.; Scheer, V.; Vogt, R.; Zellner, R. *J. Phys. Chem. A* **2000**, *104*, 819.

(10) Hanisch, F.; Crowley, J. N. *J. Phys. Chem. A* **2001**, *105*, 3096.

(11) Judeikis, H. S.; Stewart, T. B.; Wren, A. G. *Atmos. Environ.* **1978**, *12*, 1633.

(12) Barney, W. S.; Finlayson-Pitts, B. J. *J. Phys. Chem. A* **2000**, *104*, 171.

(13) Goodman, A. L.; Underwood, G. M.; Grassian, V. H. *J. Geophys. Res.- Atmos.* **2000**, *104*, 29053.

(14) Underwood, G. M.; Miller, T. M.; Grassian, V. H. *J. Phys. Chem. A* **1999**, *103*, 6184.

(15) Goodman, A. L.; Li, P.; Usher, C. R.; Grassian, V. H. *J. Phys. Chem. A* **2001**, *105*, 6109.

(16) Underwood, G. M.; Li, P.; Al-Abadleh, H.; Grassian V. H. *J. Phys. Chem. A* **2001**, *105*, 6609.

(17) Li, P.; Perreau, K. A.; Covington, E.; Carmichael, G. C.; Grassian, V. H. *J. Geophys. Res. Atmos.* **2001**, *106*, 5517.

(18) Fenter, F. F.; Francois, F.; Rossi, M. J. *Rev. Sci. Instrum.* **1997**, *68*, 3180.

(19) Koch, T. G.; Fenter, F. F.; Rossi, M. J. *Chem. Phys. Lett.* **1997**, *275*, 253.

(20) Koch, T. G.; van der Bergh, H.; Rossi, M. J. *Phys. Chem. Chem. Phys.* **1999**, *1*, 2687.

(21) Masel, R. *Principles of Adsorption and Reaction on Solid Surfaces*; John Wiley and Sons: New York, 1996; p 381.

(22) Ghopsal, S.; Hemminger, J. C. *J. Phys. Chem. A* **1999**, *103*, 4777.

(23) Atkins, P. *Physical Chemistry*, 6th ed.; W. H. Freeman and Co.: New York, 1998; p 754.

(24) For large $\gamma > 10^{-3}$, a normalization factor of $(1 - \gamma)^n$ needs to be included to ensure that the calculated observed uptake coefficient never exceeds a value of 1.

(25) Crank, J. *The Mathematics of Diffusion*, 2nd ed.; Clarendon Press: Oxford, U.K., 1975.